JOURNAL OF MATERIALS SCIENCE 24 (1989) 2756–2760

Laser-induced internal cracks in LiF single crystals

ZHAN-YI WANG, MARTIN P. HARMER, YE T. CHOU
Department of Materials Science and Engineering, and Materials Research Center, Lehigh University, Bethlehem, Pennsylvania 18015, USA

Internal cracks were generated in LiF single crystals using a focused short-pulse laser. The laser-induced fracture region is composed of a central damage zone of fragmentation and three orthogonal penny-like cracks which consist of an intermediate zone and a circumferential fracture zone. The detailed features are examined by optical and scanning electron microscopy (SEM). Mechanisms of the fracture process are discussed. The method is applicable to other transparent crystals.

1. Introduction

The destructive effects produced by focusing the radiation of a laser beam on to the surface or into the interior of a solid material have been reported by several investigators [1–5]. Hercher [1] reported that a focused laser beam could induce permanent damage in glasses and estimated that the temperature reached at the focus point of the laser beam could reach 5000 K. Field and Zafar [2] studied in detail the effects of surface thin films (carbon, metals and organic liquids) on laser damage of glass substrates. More recently, Endert and Melle [3] used X-ray topography to study laser-induced damage in nonlinear potassium dihydrogen phosphate crystals and Gorbunov *et al.* [4] studied the dislocation structure and residual stress fields around the damage zone caused by laser radiation in NaCl single crystals. However, little attention has been paid to high-energy damage in irradiated crystals where cracking initiates from the damage zone.

In studying crack healing, crack growth/closure, and the related phenomena of surface energy and surface diffusion, etc., environmental contamination is a critical factor. A key prerequisite in such studies is the formation of internal surfaces that are free from contamination. One possible method of generating clean internal surfaces is to initiate internal cracks by well-controlled laser damage. In the present paper, we describe a preliminary study of the formation of laser-induced internal cracks in LiF single crystals. These internal cracks are currently being exploited in an ongoing study of crack healing and related phenomena. The method may also be used to study other transparent crystals, such as sapphire, ruby, periclase etc.

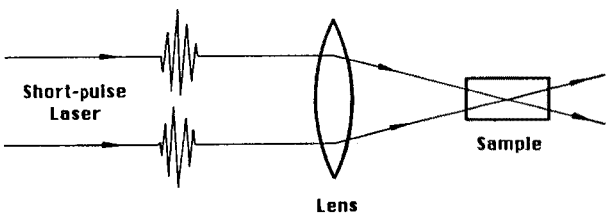

Figure 1 Schematic drawing of the experimental arrangement.

2. Experimental observations

The materials used in the present work were LiF single crystals (supplied by the Crystal Growth Laboratory, University of Utah, USA). The crystals were radiation-hardened so that they could be cleaved easily without introducing an undue number of dislocations. The size of the specimen was about 10 mm × 5 mm × 3 mm. A Nd–YAG short pulse laser (a Quanta Ray DCR-11 Pulsed Nd–YAG Laser unit, Spectra-Physics, Mountain View, California, USA) with wavelengths 1064 and 532 nm and a pulse width at half maximum of 8 nsec, was focused at the interior of a specimen through a 47 mm focal length lens (Fig. 1). The energy output of the laser pulse is about 50 mJ. After irradiation with a single pulse, fracture regions were generated at several randomly distributed spots along the beam path within the specimen as shown in Fig. 2. Each laser-induced fracture region is composed of a central damage zone and three orthogonal penny-like cracks extending from the damage zone along the {1 0 0} planes (Figs 3a to c). The dimensions of the damage zones and the cracks were 0.01 to 0.15 mm and 0.1 to 1.5 mm, respectively. A pulse with a higher

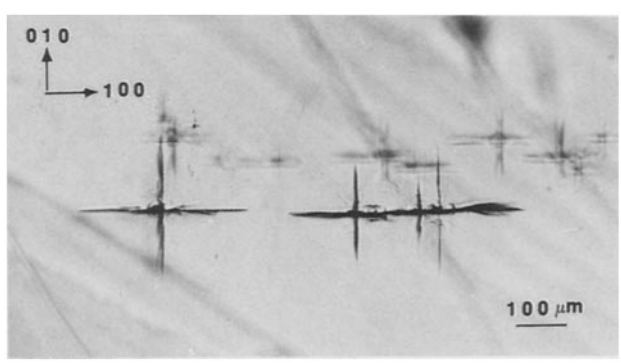

Figure 2 Transmitted optical micrograph showing the laser-induced internal cracks. Laser beam in the [1 0 0] direction.

0022–2461/89 $03.00 + .12

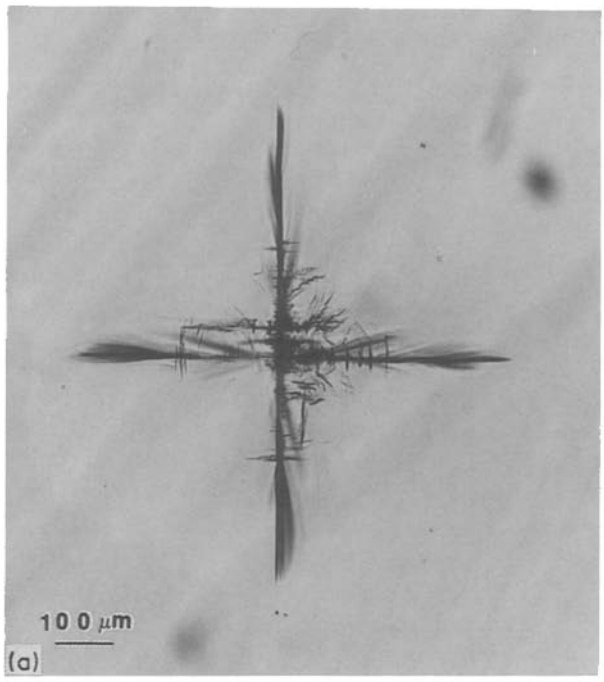

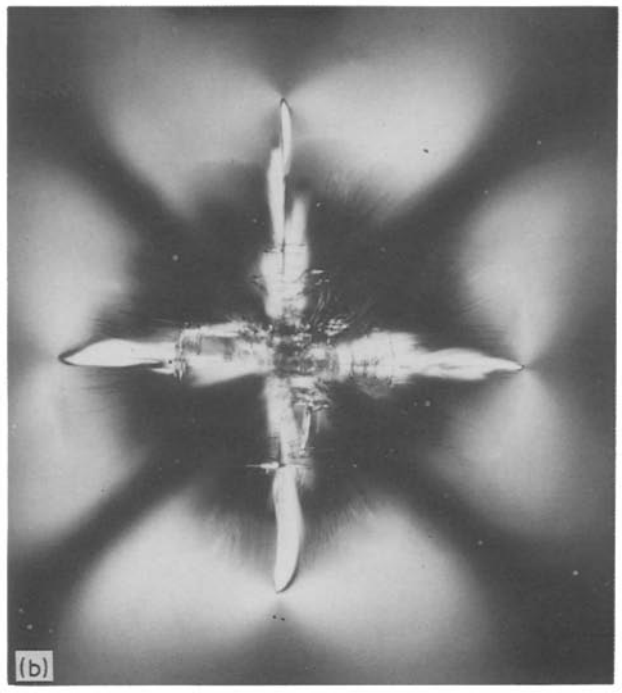

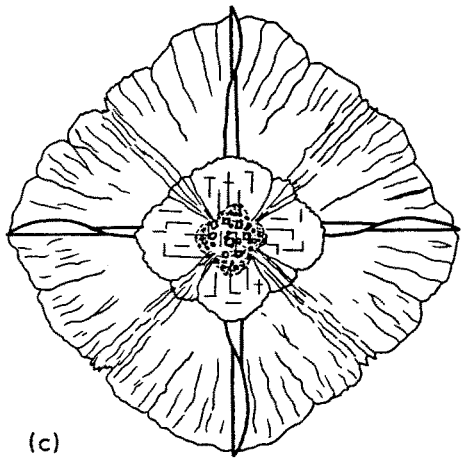

Figure 3 Laser-induced fracture region in an LiF single crystal. (a) Transmitted optical micrograph; (b) polarized optical micrograph; (c) schematic drawing.

energy output (> 50 mJ) would cause the specimen to cleave in halves.

Detailed features of the fracture region are shown in the scanning electron micrograph (Fig. 4) taken on the fracture surface after the crystal has been bend-fractured along one of the penny-like cracks. The characteristics of the central damage zone depend on the amount of energy absorbed. The damage zone generated by a highly absorbed energy contains voids and markings characteristic of the liquid flow prior to solidification (Fig. 5a). The traces of solidified melt extend beyond the damage zone into the induced crack surface (Fig. 5b). In contrast, the damage zone generated by a lower absorbed energy shows disrupted, fragmented features with many short straight cleavage cracks along the $\langle 100 \rangle$ directions (Fig. 6). Away from the damage zone, each penny-like crack consists of an inner deformation zone and an outer circumferential fracture zone. The latter, with abundant river-patterns on the fracture surface, has a typical cleavage feature and is deflected near the intersections with the other two orthogonal penny-like cracks and becomes tortuous.

The irregular intermediate zone is located between the damage zone and the circumferential cleavage surface. It usually appears in a larger penny-like crack (> 0.1 mm) and is not as pronounced in a smaller crack. The inner portion of this intermediate zone features cavities and solidification markings with growth ledges (Figs 7a and b). The cavities become smaller the further they are from the centre. The outer portion of this zone shows the characteristics of a more regular cleavage fracture. The cleavage process is arrested at the serrated boundary of the intermediate zone and a secondary cleavage process starts from this boundary. There are also many short, straight cleavage cracks along the $\langle 100 \rangle$ directions (Fig. 7a). The

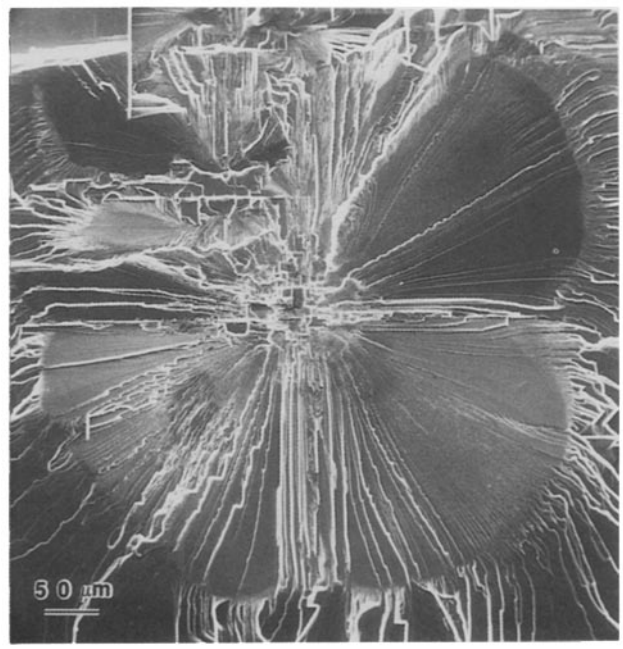

Figure 4 Scanning electron micrograph of a laser-induced penny-like crack.

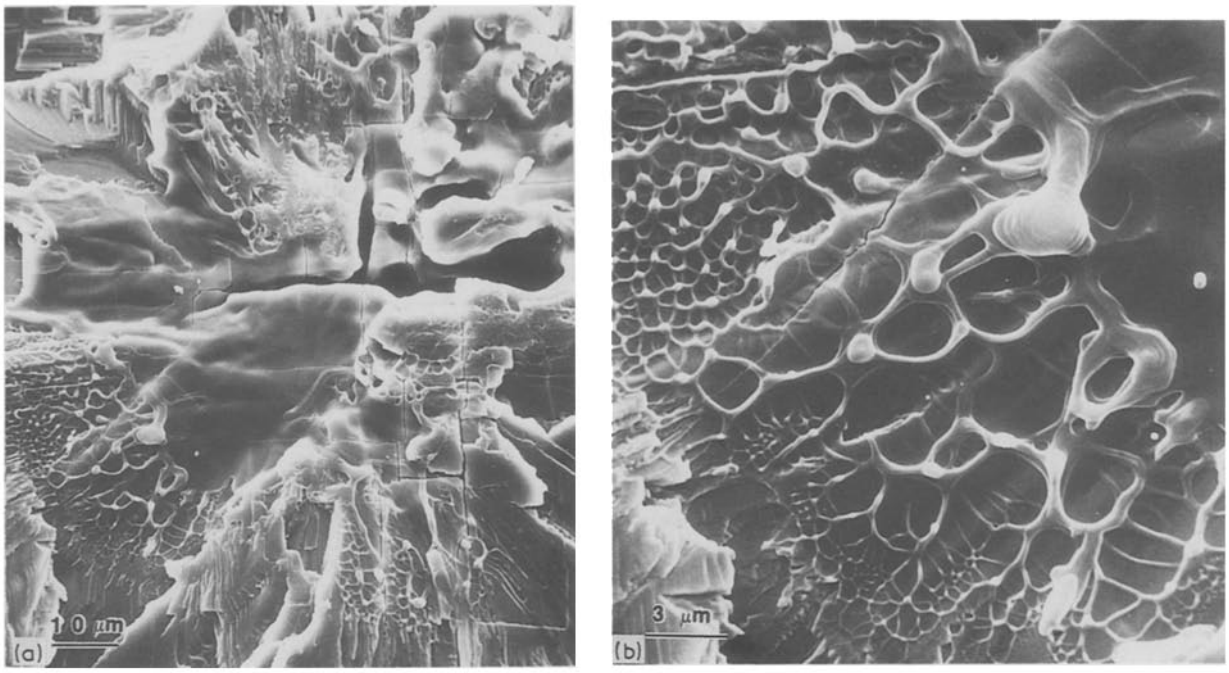

Figure 5 (a) Scanning electron micrograph of damage zone generated by a highly absorbed energy. (b) Melt intrusion into the crack surface and on-site solidification.

intermediate zone also is depicted in the polarized optical micrograph (Fig. 3b). The appearance of the stress birefringence observed with crossed nicols indicates the existence of a substantial residual stress intensity in the surrounding matrix. It is interesting to note that the stress birefringence in the surrounding matrix of the laser-induced internal crack system is similar to that of the half-penny-like radial/median crack system in a semi-infinite matrix of soda-lime glass generated by a Vickers indentation [6, 7].

The fracture surface was etched with a solution of 49 ml HF, 49 ml glacial acetic acid and 2 ml HF saturated with FeF_2 [8]. Dislocations were revealed around the laser-induced fracture region on the etched surface (Fig. 8). A high density of dislocations was generated in the vicinity of the damage zone, together with dislocation bands extended along the $\langle 1\,1\,0 \rangle$ directions. These observed dislocation structures are similar to those observed in the NaCl crystals [4]. Also observed are the sets of edge-type blunting dislocations generated sequentially from the growing crack tip. These blunting dislocations are distributed on the $\{1\,1\,0\}$ planes 45° from the $\{1\,0\,0\}$ cleavage plane, forming a shielding zone in front of the induced crack.

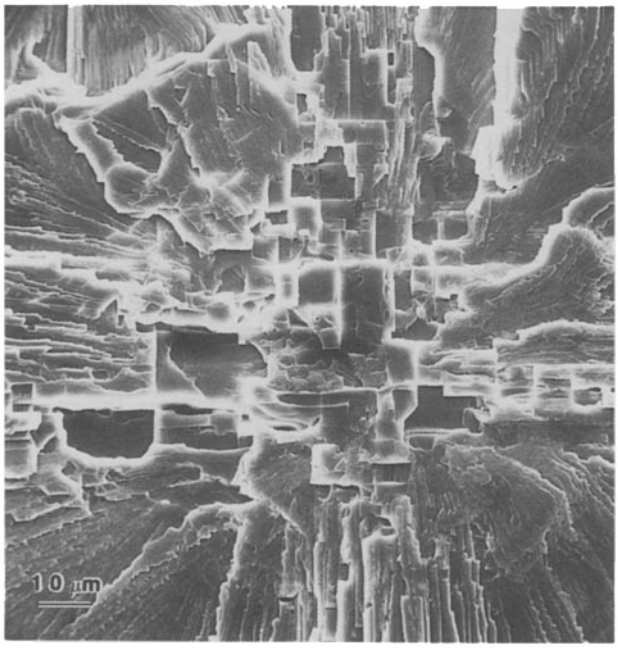

Figure 6 Scanning electron micrograph of damage zone generated by a lower absorbed energy.

3. Discussion

Based on the morphology of the fracture regions, it is suggested that the laser-induced fracture is a thermal spike process. In the volume irradiated by the focused laser beam, an intense local absorption had occurred at the optical inhomogeneities. A simple calculation indicates that the power density of the laser pulse can reach $\sim 3\,\mathrm{MW\,cm^{-2}}$ (the power of the laser beam is about 50 mJ/8 nsec $= 6 \times 10^6$ W and the diameter of the beam focus is about 0.05 cm). If a small portion of this power were to be absorbed at the inhomogeneities, the nearly adiabatic heating could raise the temperature in these regions to a value much higher than the melting and vaporization temperatures of the material. The sudden volume expansion of the superheated liquid/vapour exerted a compression impulse on the surrounding matrix. The resulting thermal stress thus generated a high density of dislocations in the vicinity of the damage zone, which then glided away at a high speed in the $\langle 1\,1\,0 \rangle$ directions [4]. In addition, the strain built up in the matrix was released by generating crack surfaces along the weakest $\{1\,0\,0\}$ planes in the intermediate deformation zone. As seen in Fig. 5b, some of the melt intruded inside the root of the cracks. During cooling of the superheated liquid, the intruded melt solidified on-site due to a faster cooling rate at the front and formed the observed distribution of cavities and solidification markings.

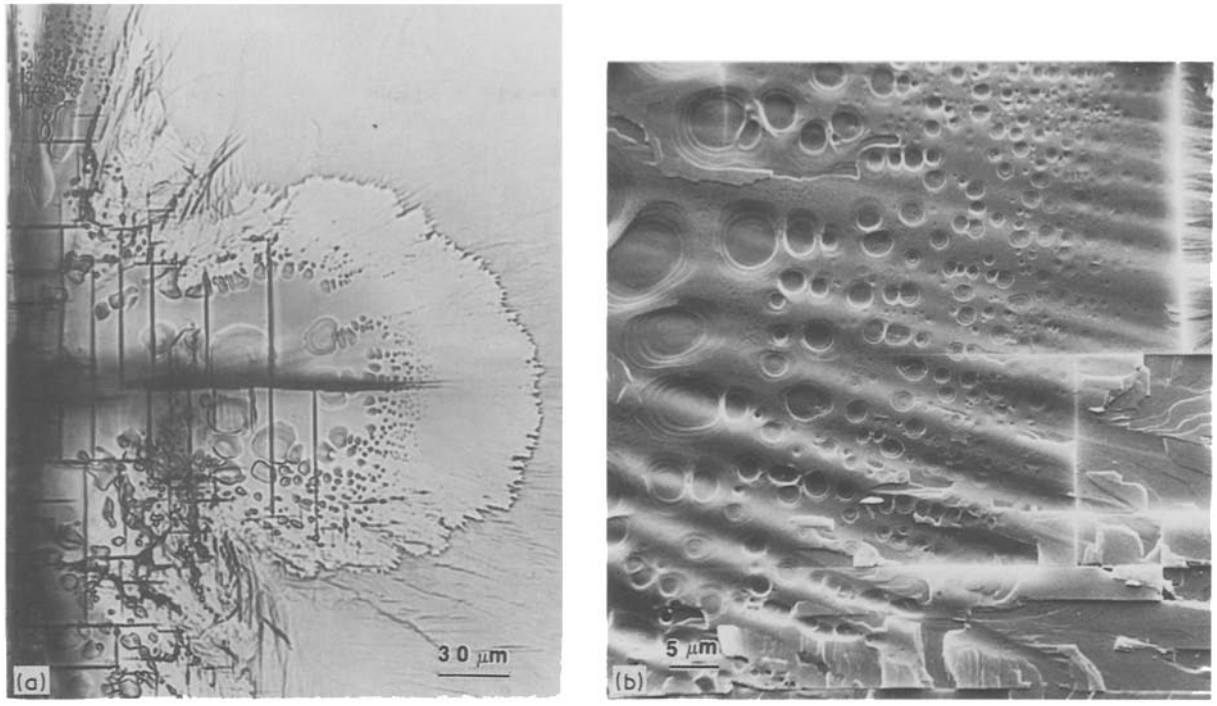

Figure 7 Intermediate deformation zone. (a) Transmitted optical micrograph; (b) scanning electron micrograph.

Upon cooling, the volume contraction of the superheated liquid could not be accommodated by the surrounding matrix due to the irregular solidification and fragmentation. Thus, the mismatch of the damage zone and the surrounding matrix caused a residual stress in the matrix which effectively wedged open the secondary circumferential cleavage planes (starting at the serrated boundary of the intermediate zone). If one considers the similarity between the present situation and a point load in the indentation analogue, it is suggested that the residual stress would vary as the inverse square of the radial distance from the damage zone [9]. Furthermore, the local stress intensity at the crack tip would be shielded by the blunting dislocations. These two effects then limited the cleavage fracture to its final size, which was reached when the residual stress intensity at the crack tip dropped below the threshold value for crack extension. Chia and Burns [10] observed blunting dislocations ahead of a wedge-opening crack tip in a LiF single crystal (see Fig. 3 in [10]). Because the crack extension rate used was relatively slow, only a few blunting dislocations appeared near the final crack tip. In the case of laser-induced cracking, the crack extension rate was much faster. A large number of blunting dislocations was sequentially generated while the crack was extending, thus forming an extensive shielding zone in front of the crack.

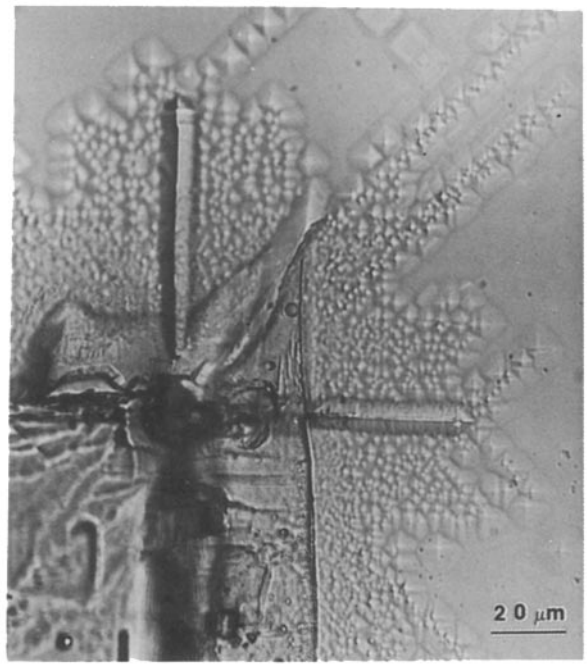

Figure 8 Dislocation etch pits on the fracture surface in the laser-induced fracture region.

It is worth pointing out that the mechanical effect of the local superheating/cooling cycle is analogous to that of the loading/unloading cycle during the indentation deformation [11]. Under indentation, a residual contact stress is built up by the mismatch between the irreversible plastic deformation zone and the elastic matrix. Similarly, in a laser-induced fracture process the residual contact stress stems from the mismatch of the irreversible damage zone and the surrounding matrix. This explains the similarity of the stress birefringences between the two fracture systems.

4. Conclusions

1. Internal cracks are generated in LiF single crystals by a focused short-pulse laser with controlled power.
2. The laser-induced fracture region is composed of a central damage zone and three orthogonal penny-like cracks along the {1 0 0} planes. Each penny-like crack consists of an intermediate zone and a circumferential fracture zone.
3. The characteristics of the central damage zone depend on the energy absorbed at the optical inhomogeneities in the crystal.
4. Edge-type blunting dislocations are sequentially

generated from the crack tip and form a shielding zone in front of the laser-induced crack.

Acknowledgements

The authors thank Dr B. R. Lawn and G. A. Miller for helpful discussions. We also thank Professor J. P. Huennekens for his permission to use the Nd–YAG laser unit and Dr B. K. Clark for expert technical assistance. This work was supported by the National Science Foundation under Grant No. DMR-8352013.

References

1. M. HERCHER, *J. Opt. Soc. Amer.* **54** (1964) 563.
2. J. E. FIELD and M. A. ZAFAR, *J. Phys. D Appl. Phys.* **5** (1972) 2105.
3. H. ENDERT and W. MELLE, *Phys. Status Solidi (a)* **74** (1982) 141.
4. A. V. GORBUNOV, E. M. NADGORNYI and S. N. VAEKOVSKII, *ibid.* **66** (1981) 53.
5. NBS Special Publication (US), 727, Laser Induced Damage in Optical Materials (1984).
6. D. B. MARSHALL and B. R. LAWN, *J. Mater. Sci.* **14** (1979) 2001.
7. D. H. ROACH and A. R. COOPER, *J. Amer. Ceram. Soc.* **68** (1985) 632.
8. J. J. GILMAN, *Trans. AIME* **209** (1957) 449.
9. B. R. LAWN and M. V. SWAIN, *J. Mater. Sci.* **10** (1975) 113.
10. K. Y. CHIA and S. J. BURNS, *Scripta Metall.* **18** (1984) 467.
11. B. R. LAWN and T. R. WILSHAW, *J. Mater. Sci.* **10** (1975) 1049.

Received 21 June
and accepted 14 November 1988